Universidad de La Laguna

Facultad de Ciencias
Sección de Física

TRABAJO DE FIN DE GRADO

Formation and evolution of galaxies in cold dark matter cosmology

Elena Arjona Gálvez

Supervisores:

Dr. Claudio Dalla Vecchia
Dr. Chris Brook

Contents

Resumen **i**

1 Introduction **1**
1.1 Classifications of galaxies: The Hubble sequence. 1
1.2 Formation and evolution of galaxies 2

2 Objectives and Methodology **5**
2.1 Objectives 5
2.2 Methodology 6

3 The data **7**
3.1 The EAGLE simulations 7
3.2 Sample selection 9

4 Results **13**
4.1 Number of satellites per galaxy host 13
4.2 Visual insight of the galaxy host 19

5 Conclusions **27**

6 Bibliography **29**

Resumen

El estudio de la evolución y formación de galaxias es una de las mayores líneas de investigación abiertas en la astrofísica hoy en día. Entender cómo se han formado, su morfología y cómo han cambiado con el tiempo supone un gran paso para el conocimiento del universo actual. Existen diversas teorías que explican la evolución de las galaxias, la más aceptada afirma que se debe, en gran medida, a un proceso de fusión entre ellas. Estos procesos son tan violentos que, durante la fusión, las estrellas y la materia oscura pertenecientes a cada galaxia se ven afectados por un fuerte potencial gravitatorio, consiguiendo incluso que cambien su morfología. Así, si dos galaxias chocan entre ellas, se produce un proceso de fusión en el cual todo el movimiento orbital existente anteriormente entre las estrellas de cada galaxia se convierte en un proceso aleatorio de energía produciendo que estas estrellas, que antes de la fusión poseían un movimiento ordenado, pasen a orbitar de manera completamente aleatoria, lo que produce una galaxia de tipo elíptico.

Para explicar esto, [Ruiz et al., 2015] realizó, mediante datos recogidos observacionalmente, un estudio sobre el número de satélites existentes en galaxias de tipo masivo y la dependencia de éstos con la morfología de la galaxia. En este caso, encontró que, para un rango de masa entre 10^{11} $M_{\odot}$ y 210^{11} $M_{\odot}$ las galaxias elípticas poseían mayor número de satélites seguidas de las galaxias de tipo lenticular y finalmente, las galaxias de tipo espiral. Este hecho pone en acuerdo la teoría de la fusión de galaxias como el canal más probable de evolución.

Nuestro trabajo consistirá en reproducir el trabajo realizado por [Ruiz et al., 2015] mediante simulaciones de galaxias. Para ello, utilizaremos EAGLE, un conjunto de simulaciones hidrodinámicas desarrolladas por el Virgo Consortium. Dichas simulaciones, gracias a la enorme variedad de procesos físicos que incluyen, son una poderosa herramienta para los físicos con la que poder entender los distintos mecanismos físicos que se producen en el universo.

Al principio del proyecto extraeremos de EAGLE todas las galaxias centrales, a redshift cero, que pertenecen a un halo galáctico con una masa en estrella mayor de 10^{11} $M_{\odot}$ y, por otra parte, las galaxias satélites de este halo con una masa en estrella mayor de 10^{9} $M_{\odot}$. Seguidamente, mediante diversos procesos se unirán los satélites a sus galaxias centrales y se separarán estas últimas en referencia a su morfología. Tras esto, se realizará un estudio minucionso de la dependencia del número de satélites en relación con la morfología de la galaxia central, primero con el rango de masa utilizado en [Ruiz et al., 2015] y luego con todas las galaxias centrales masivas extraídas comparando así los resultados observacionales con las simulaciones.

Nuestro trabajo está estructurado de la siguiente manera. En el capítulo 1 realizaremos un planteamiento teórico del tema a tratar en nuestro trabajo con el objetivo de introducirlo en nuestro trabajo. Seguidamente, en el capítulo 2 se expondrán brevemente los objetivos y la metodología seguida a lo largo de nuestro proyecto. En el capítulo 3 realizaremos una detallada explicación de EAGLE y su modo operandi. Por último, en los capítulos 4 y 5 se expondrán los resultados y las conclusiones obtenidas así como los posibles trabajos futuros.

Chapter 1

Introduction

En el universo existen galaxias las cuales, debido a sus diferencis, podemos clasificar en distintos grupos. En 1926, Hubble propuso una clasificación basada en su forma. En esta clasificación, las galaxias podrían ser elípticas, lenticulares, disco o irregulares dependiendo de distintos factores. Tras ello, muchas han sido las teorias y conjeturas de los astrofísicos para entender cómo las galaxias han llegado a tener esta forma y cómo se han desarrolado a lo largo del tiempo.

1.1 Classifications of galaxies: The Hubble sequence.

Many schemes for classifying galaxies have been developed over the years. In 1926, Hubble proposed a morphological classification scheme for galaxies based essentially on their brightness [Hubble, 1926]. In this classification, various types of galaxies are divided into three main groups: elliptical, lenticular and spiral galaxies. These last are separated into two sequences: normal and barred spiral. Furthermore, for all galaxies that do not follows the scheme above, Hubble included a class of irregular galaxies.

In the Hubble sequence, there is little interstellar matter in the elliptical galaxies. In addition, the difference among elliptical galaxies only resides in their shape.

Lenticular or S0 galaxies can be seen as a "transition galaxy", in the sense that they do not have signs of spiral structure nor contain a significant amount of interstellar matter like the elliptical galaxies, as they have an elliptical shape but lack a disk of inner gas, that can be tipically found in spiral galaxies.

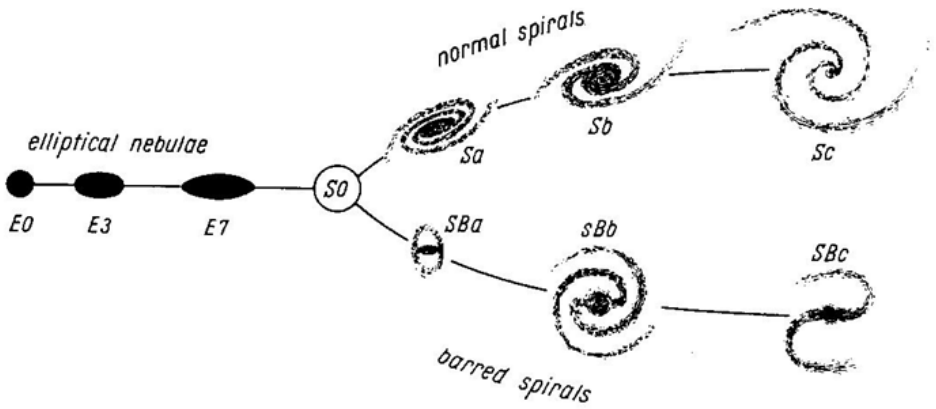

Figure 1.1: Hubble sequence.

The aspects characterising spiral galaxies are a central bulge, similar to an elliptical galaxy, and two types of discs: a stellar disc like S0 types and a disc of gas, stars and other interstellar matter which forms the spiral pattern. These discs indicate that young star are being born in this area. On one hand, the spiral pattern belonging to barred spirals galaxies ends at a central bar of the bulge, on the other hand, in normal spiral galaxies, the spiral pattern ends at an inner ring, as we can see in the figure 1.1 for the Sa, Sb types, or ends right at the centre, like for the Sc type.

1.2 Formation and evolution of galaxies

When choosing the location for galaxies to form the first method that comes to mind would be the examination of the structures of the universe. Because of gravity interactions, we can distinguish some clear structures such as filaments, voids, dark matter haloes of galaxies and clusters of galaxies.

Within a specific halo, one can generally differentiate the (central) main galaxy, which resides at rest at the center of its dark matter halo, and its satellites galaxies with lower mass, which orbit the halo associated with the central galaxy. If the satellite galaxy has mass enough (around 10^9 $M_\odot$) it could reside it could lies within dark matter subhaloes with its own satellites.

.

The study of galaxy formation and evolution has increasingly advanced in the last years. One of the most likely mechanisms for growth of massive galaxies, like elliptical galaxies, is galaxy mergers. Previous research supports this channel of size evolution, in which first, the bulk of the mass of the most massive galaxies were created as early as z $\approx$ 2 in an intense starburst [Kereš et al., 2005, Dekel et al., 2009, Oser et al., 2010, Ricciardelli et al., 2010, Wuyts et al., 2010, Bournaud et al., 2011], and later the envelope was developed through the merger with satellites of ancestor galaxies [Oser et al., 2010, Khochfar and Silk, 2006]. In addition, spirals galaxies have been formed due to a strong angular momentum on the halo that generates the formation of a disc. [Dressler, 1980] pointed out that there is a slow relation between density and morphological type, so that a significant number of lenticular galaxies exist in regions where gas density and temperature are too low to remove the gas from spirals by ram pressure stripping.

In addition, other authors have pointed out that the average velocity dispersion of the host galaxies has decreased mildly since $z \approx 2$, [Javier Cenarro and Trujillo, 2009], which are in accordance with the merger scenario. Otherwise, observations suggest that the growth of massive galaxies cannot depend on their intrinsic features, like their size or their stellar population age, but on other external factors [Trujillo et al., 2011, Díaz-García et al., 2013].

1.2.1 The relation between the abundance of satellites with the morphology of the host galaxy

For host galaxies, parameters like the abundance of satellites or their intrinsic properties are bound up with their host merger histories. These properties are closely correlated with the underlying cosmology and they can be used to establish useful constrains to the models. The main goal of the study realised by [Ruiz et al., 2015] is the analysis of the relation between the abundance of satellites around 254 masive galaxies, ($10^{11}M_{\odot}$), sorted into morphological types. They segregate their sample of galaxies in four morphological groups. Their classification identifies visually the elliptical lenticular and two types of spiral galaxies: Sa and Sb/c with the aim to explore the correlation between the number of satellites and the morphology of the host.

With their results, massive ellipticals seem to be surrounded by a remarkably larger number of massive satellites whereas the rest of morphological types typically merge with

more massive objects. They also obtain for the lenticular and spirals types that the main contributor to the evolution of massive spirals seem to be the most massive satellites. For ellipticals, the merger channel ais in agreement with the results pointed by [Oser et al., 2012]

Their work highlights the importance of the environment where massive galaxies are immersed and how that the host morphology is strongly linked to the environment.

Chapter 2

Objectives and Methodology

Nuestro objetivo es estudiar si existe una dependencia entre el número de satélites de una galaxia central y su morfología, para ello utilizaremos galaxias obtenidas mediante simulaciones. Para llevar a cabo este estudio, separaremos las galaxias de las simulaciones en dos tipos: galaxias centrales y galaxias satélites. Después, por un lado realizaremos un tratamiento separando las galaxias centrales en tres tipos: elípticas, lenticulares y espirales y por otro uniremos cada galaxia central a sus galaxias satélites correspondientes para estudiar la diferencia existente entre el número de satélites y la morfología de cada una.

2.1 Objectives

The main objective of this project is to prove the dependence of the amount of satellites with the morphological types of host galaxies of the same mass. To do this, we are going to select all central galaxies within the EAGLE cosmological simulation that have a stellar mass larger than 10^{11} $M_{\odot}$.

This *trabajo de fin de grado* serves to provide a deeper insight into the study carried out by [Ruiz et al., 2015] about the relationship between the morphology of massive galaxy hosts and their number of satellites using observational data. In the course of this work, we are going to analyse the differences between the results that have been obtained through observational data, [Ruiz et al., 2015], and our results using simulations.

2.2 Methodology

In order to carry out this work, we are going to use an hydrodynamical simulation of EAGLE, with intermediate resolution. Thanks to the tools that will be explained in section 3.1, we will be able to study if a distinction between the central galaxies and their satellites is possible.

Every central galaxy with a mass larger than 10^{11} $M_{\odot}$ will be treated as a host galaxy, and later sorted into morphological classes according to the scheme established by [Sales et al., 2010] and [Romanowsky and Fall, 2012] based on the rotational velocity and the central bulge of the galaxy.

On the other hand, we are going to considered only satellite galaxies with a mass larger than 10^{9} $M_{\odot}$ and, through various mechanisms developed in the section 3.2.2, we are going to link this satellites with their respective host.

Once the central galaxies are sorted by morphology and linked to their respective satellite galaxies, it is possible to obtain for each galaxy the total number of satellites that they have and the ratio of satellite to central galaxies. With these data, we are going to reproduce the analysis done by [Ruiz et al., 2015] to study the morphological dependence of galaxies and their number of satellites.

A detailed explanation of how EAGLE database works and how to establish the relationship between satellites and host galaxies is given in the following section, 3.1.

Chapter 3

The data

En este capítulo realizaremos una detallada explicación de EAGLE y su funcionamiento. Primero veremos el motivo y la necesidad de llevar a cabo un proyecto tan ambicioso como EAGLE y, tras ello, explicaremos el procedimiento que hemos seguido a la hora de obtener nuestras galaxias centrales y de unirlas con sus respectivos satélites. Se planteará también el modo de clasificación que hemos seguido para los distintos tipos morfológicos.

3.1 The EAGLE simulations

To study the assembly and evolution of galaxies, rigorous techniques need to be developed to test the different theories. The physical and astrophysical phenomena behind this have a highly non-linear behavior, making analytical description hard to reach. For this reason, the use of numerical simulations has improved our understanding of cosmological events.

One of the most important tools that can be used to model galaxies and, simultaneously, the intergalactic medium (IGM), is cosmological hydrodynamical simulations. This allows us to achieve a better understanding about the feedback cycles and fuelling of different types of galaxies. If the similarities between observations and hydrodynamical simulations of galaxy formations are sufficiently strong, the simulations can be used to calculate cosmological and physical parameters that we could not measure only with observations, [Croft et al., 1998, Schaye et al., 2000, Viel et al., 2004, McDonald et al., 2005].

With this objetive in mind, the Virgo Consortium has developed the "**E**volution and **A**sembly of **G**a**L**axies and their **E**nviorments" (hereafter EAGLE) project for cosmological supercomputer simulations [Schaye et al., 2015, Crain et al., 2015]. EAGLE simulations consist of a suit of cosmological hydrodynamical simulations in which the main models were run in cubic, periodic volumes with length of 12, 25, 50, and 100 comoving Mpc (cMpc), designed to reproduce the evolution and formation of galaxies, i.e, to track the evolution in time from a redshift of z = 127 to the present day of baryonic and non-baryonic matter. This can be possible through the calibration of a limited subset of $z = 0$ observations of galaxies, such as the stellar mass function of galaxies, the sizes of galaxies and the correlation between stellar mass and black hole mass.

All simulations use a modified version of the GADGET-3 Tree-SPH, N-body Tree-PM smoothed particle hydrodynamic code based on the GADGET-2 code, that includes the implementation of a large number of subgrid modules that supply physical processes with a limited resolution scale, described by [Schaye et al., 2015], such as stellar evolution, star formation, metal enrichment, feedback from star, the feedback generated by merging and accretion of supermassive black holes, etc.

The EAGLE simulations adopt a flat ΛCMD cosmology with the parameters listed below, determined by the Planck Collaboration [Ade et al., 2014]. The initial condition have been generated using second-order Lagragian perturbation theory [Jenkins, 2010].

Ω_Λ	Ω_m	Ω_b	σ_8
0.693	0.307	0.04825	0.8288
n_s	Y	H_0 [km s^{-1} Mpc^{-1}]	
0.9611	0.248	67.77	

In this work we use RefL0100N1504, an hydrodynamical simulation with a force resolution of 0.7 pkpc which we refer to as intermediate resolution. This simulation is the largest of EAGLE, with a comoving box size of 100 Mpc and 1504^3 dark matter particles (being at the initial time the same number of baryonic particles). In addition, this simulation has a mass resolution of 1.81×10^6 $M_\odot$ for gas particles and 9.70×10^7 $M_\odot$ for dark matter particles [McAlpine et al., 2016]. The resolution is high enough to allow for comparisons with observations of global galaxy properties.

3.2 Sample selection

For each EAGLE simulation, the respective catalogue of galaxies has been distributed in SQL tables. We are going to use the **FOF**, **SubHalo** and **MorphoKinem** tables which provide us all the required information for the development of our work.

The information contained in **FOF** SQL table has been obtained through the *friends-of-friends* method [Davis et al., 1985, Summers et al., 1995] to identify the particles in the different halos in the simulation. This method is used to establish a minimum separation between particles, named linking length (h_{link}), and identify all particles inside them. These particles are designated *friends* and the halo consist of a suit of particles connected one by one or more across these relations, i.e., *friends-of-friends*. They also use spherical over-density algorithms [Springel et al., 2001, Dolag et al., 2009] to identify the density threshold that can be parameterized as the linking length as follow:

$$h_{link} \approx 0.2\langle \Delta x \rangle = 0.2\sqrt[3]{\frac{V}{N}} \tag{3.1}$$

where N is the total number of particles and V is the volume of our simulation.

Then, the particles belonging to the same halo have been labelled with the group ID, *GroupNumber*. Also, particles with their own bound structure are labelled with a subgroup identifical by *SubGroupNumber* in the database, where 0 is the *SubGroupNumber* of the main galaxy, or host, in the **FoF** group, [Schaye et al., 2015, The EAGLE team, 2017, McAlpine et al., 2016].

3.2.1 Sample selection of host galaxies

In order to reproduce the work of [Ruiz et al., 2015] with the objetive of discussing the similarities and differences between the observations and the simulations, we have extracted from EAGLE a number of massive galaxies with their respective satellites. For the sample selection of central galaxies, we are going to select in the simulation all host galaxies with a stellar mass larger than 10^{11} $M_{\odot}$, and with the aim to select only the host galaxies, we also have imposed a *SubGroupNumber* equal to zero, which means we are only analysing central galaxies. The selection criteria corresponds to 262 massive galaxies at $z = 0$.

For the halo properties we use the **FoF** field. In addition, for all parameters belonging to the own host galaxy (such as the stellar mass, the distance, etc.) and its morphology (like the relation between the brightness of the host galaxy bulge per total luminosity) we use the **Subhalo** and **Morphokinem** tables. Once all massive host galaxies have been selected, we can link the different tables using the *GroupID* (**FoF** and **Subhalo** tables) and the *GalaxyID* (**Subhalo** and **MorphoKinem**) parameters in order to extract the features of each host galaxy.

In addition, a fourth field has been provided by Dr. Claudio Dalla Vecchia in order to add the rotational kinetic energy and the parameters refering to the size of the galaxies. This information has been connected to the above list via the same GroupNumber and a SubGroupNumer.

3.2.1.1 Sorting the host galaxy into morphological classes

With the main objective of making a morphological classification of all the central galaxies from the simulation, we have taken into account different factors.

Firstly, we have sorted the galaxies in two types —passive galaxies and star forming galaxies, depending on their star formation activity. For make this classification, EAGLE compute the star formation rate through the method implemented by [Schaye and Dalla Vecchia, 2008] in addition with the metallicity-dependent density threshold from [Schaye, 2004]. For each gas particle, the star formation rate is given by the following equation:

$$\mathrm{SFR} = \dot{m}_{i,*} = m_{i,g} A (1 M_{\odot} pc^{-2})^{-n} (\frac{\gamma}{G} f_g \bar{P})^{(n-1)/2} \tag{3.2}$$

where m_g is the mass of gas particle, γ is the ratio of specific heats (equal to 5/3), G is the universal gravitational constant, f_g is the ratio of gas and total baryonic mass of the halo and $\bar{P}$ is the total pressure. The A and n parameters are constants that have been determined by observations [Schaye et al., 2015, The EAGLE team, 2017], and in this case are equal to 1.515×10^{-4} $\mathrm{M_{\odot}\ yr^{-1}\ kpc^{-2}}$ and 1.4 respectively, [Kennicutt, Jr., 1998]. The above equation is implemented stochastically, where the probability of a gas particle colliding and creating a star particle during a time Δt is $\min(\dot{m}_* \Delta t / m_g, 1)$.

Thus, we are going to define the specific star formation rate as the fraction between the star formation rate and mass of the relevant host galaxy:

$$\text{sSFR} = \frac{\text{SFR}}{M_*} \tag{3.3}$$

With this, we have imposed a threshold to identify the two different types of galaxies. If the galaxies have a specific star formation rate larger that 10^{-11} yr^{-1}, [Schaye et al., 2015], they will be considered star forming, and those that have a lower specific star formation rate are classified as passive galaxies.

After having sorted all the central galaxies into two types according to their star forming capacity, we know that the spiral galaxies belong to the star forming galaxies and the galaxies with a elliptical and lenticular morphology are generally passive. Various researchers have classified the galaxies according to their morphological characteristics. [Sales et al., 2010] pointed out that galaxy disks can be found through their amount of rotational velocity. The amount of rotational kinetic energy is defined by the following equation as:

$$k_{rot} = \frac{K_{rot}}{K} = \frac{1}{K} \sum_{r<30kpc} \frac{1}{2} \left[L_z/mR\right]^2 \tag{3.4}$$

where K is the total kinetic energy, L_z is the projection on the total angular momentum of the angular momentum for a particle, R is the distance between the particle and the rotational axis and m the mass of the particle. Therefore, [Sales et al., 2010] established that spiral galaxies have a rotational kinetic energy larger than 0.4.

Moveover, the prominence of the bulge is one of the key ingredients in the galaxy morphological criteria. [Romanowsky and Fall, 2012] use another classification for the morphology in relation with the brightness of the bulge. In this work, having the star formation classification in mind, they made a separation with all of host galaxies that have a B/T (i.e, the ratio of the brightness of the bulge per total luminosity of the host galaxy) larger than 0.9 for ellipticals between 0.4 and 0.8 for lenticulars, and lower than 0.5 for spiral galaxies.

3.2.2 Sample selection of satellites

For the selection of satellites, and with the aim to reproduce the work of [Ruiz et al., 2015], we have considered all satellite galaxies with stellar mass larger than 10^9 $M_\odot$. The link between the satellites and their host has been done taking into account that, as we saw in section 3.2, each halo has a own number of *GroupID* and all galaxies belonging to the same halo have the same *GroupID*. In addition, we have imposed that all satellites have a *SubGroupNumber* not equal to zero.

Chapter 4

Results

En este capítulo se muestran los resultados obtenidos a lo largo de la realización de nuestro proyecto. Primero se plantea un análisis en primer orden en base a la posibilidad de que exista realmente una diferencia entre las distintas galaxias centrales, más allá de la forma de estas. A continuación se mostrarán los resultados obtenidos con las simulaciones y se compararán con los resultados observacionales. Por último, se mostrará un ejemplo visual de ls galaxias que hemos utilizado en nuestro proyecto, separadas morfológicamente.

4.1 Number of satellites per galaxy host

With the classification we have mentioned in the section 3.2.1.1 for the rotational velocity proposed by [Sales et al., 2010] and the bulge fraction, B/T by [Romanowsky and Fall, 2012], within the stellar mass range from 10^{11} $M_\odot$ to 2×10^{11} $M_\odot$ we select 33 E-type, 29 S0-type and 28 S-type galaxies[1] We have established this upper mass limit with the goal to discuss the result obtain by [Ruiz et al., 2015] within the same mass range.

In figure 4.1 we can see the distribution of host galaxies sorted by morphology. The galaxies that are not inside any coloured area have been classified like irregular galaxies and they will not be taken into account in the following results.

[1]The section 4.2 illustrates some of host galaxies for each morphological type.

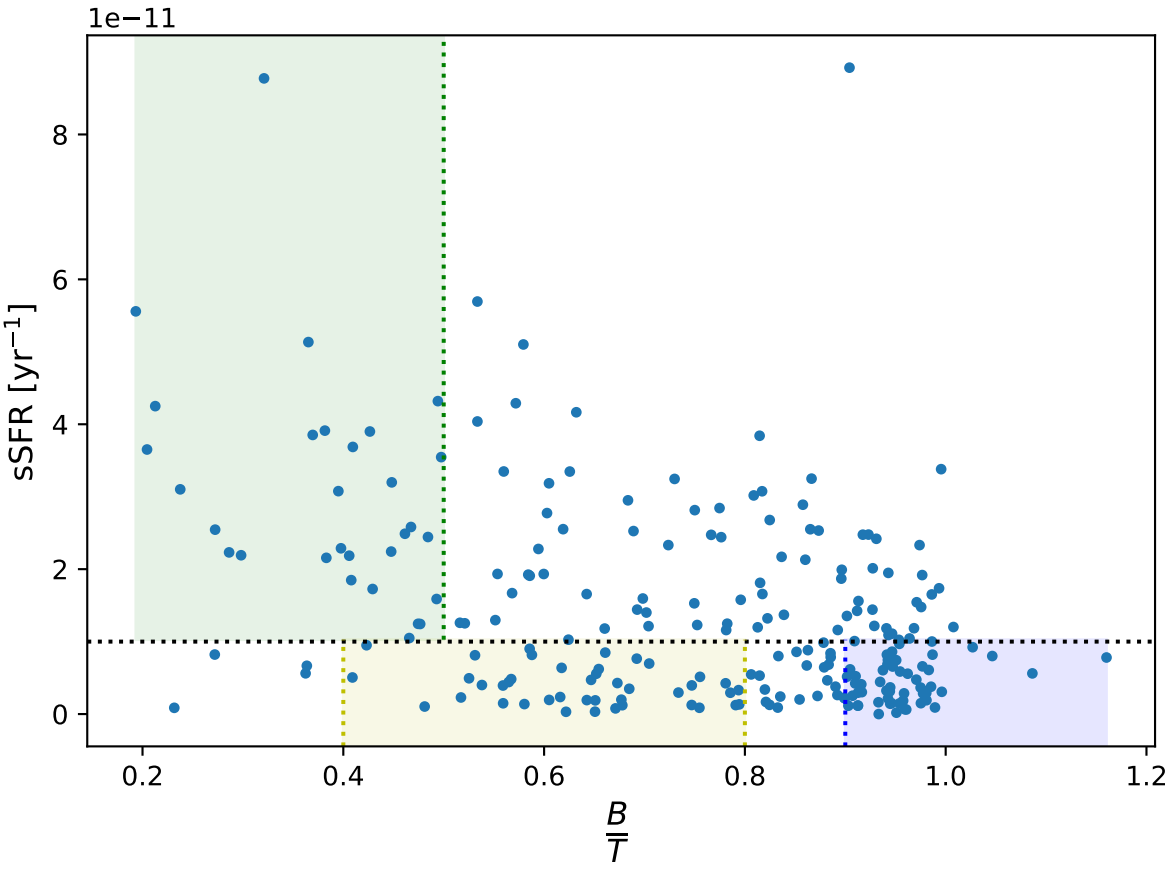

Figure 4.1: Number of host galaxy per morphology. The coloured areas represent the space of each morphological type. The **green area** corresponds to **spiral galaxies** type, the **yellow area** indicates where **lenticular galaxies** are and the **blue region** holds the **elliptical type**.

If we repeat the same procedure, but select all host galaxies with stellar mass larger than 10^{11} $M_\odot$, we get 53 elliptical galaxies, 45 lenticular galaxies and 35 spiral galaxies. A larger increase in ellipticals is expected, being the most massive galaxies in the universe of this type.

4.1.1 The dependence with the morphology of the host galaxy

In order to carry out this work, we are going to analyze all central galaxies with a stellar mass larger than 10^{11} $M_\odot$. We can check if there is, at first order, a dependence between the host morphology and the number of satellites. To accomplish this, a simple study of the correlation of the virial mass, M_{200}[2], of the halo and the number of satellites is

[2]The M_{200} of the halo is referred to the total mass within radius which density is 200 times the critical density of the Universe.

enough.

In figure 4.2 we can see that there is a strong correlation between M_{200} of all host galaxies and the number of their satellites, [Tinker et al., 2008]. This fact tells us, at first glance, that there is no dependence with the morphology, this is, they all follow the following relation:

$$\log_{10}(N_s) = \alpha \log_{10}(M_{200}) + \log_{10}(A) \tag{4.1}$$

where α is the slope of the linear relation and $\log_{10}(A)$ is the y-intercept.

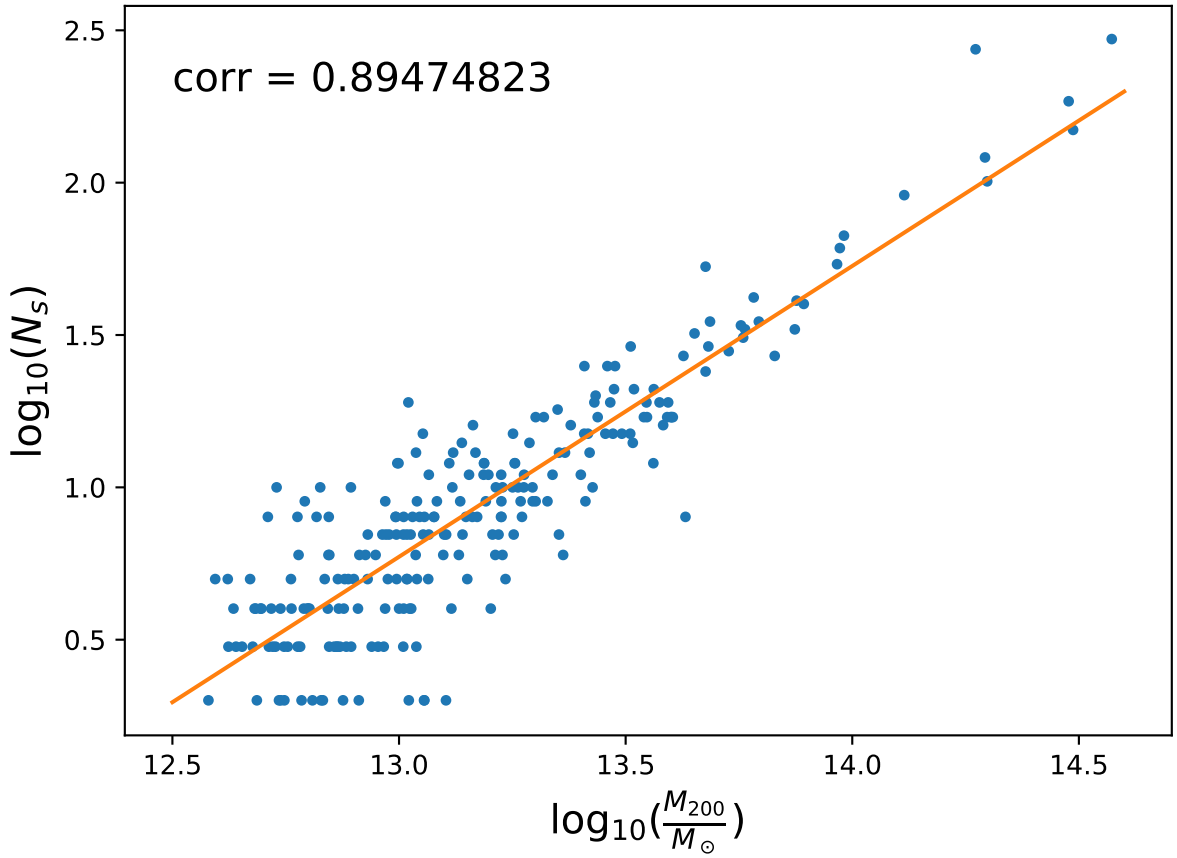

Figure 4.2: Correlation between M_{200} and the number of their satellites

In addition, we repeat the same procedure, but this time with different morphological types. If we take into account the relative error of each morphological type in relation to all host galaxies, we can not see a significant differences (figure 4.3). The

three types are closed enough and owns a certain error for us to be able to deem a difference.

	Elliptical type	Lenticular type	Spiral type
α	1.02 ± 0.06	0.92 ± 0.04	0.81 ± 0.14
$\log_{10}(A)$	-12.5 ± 0.9	-11.2 ± 0.5	-9.8 ± 1.8

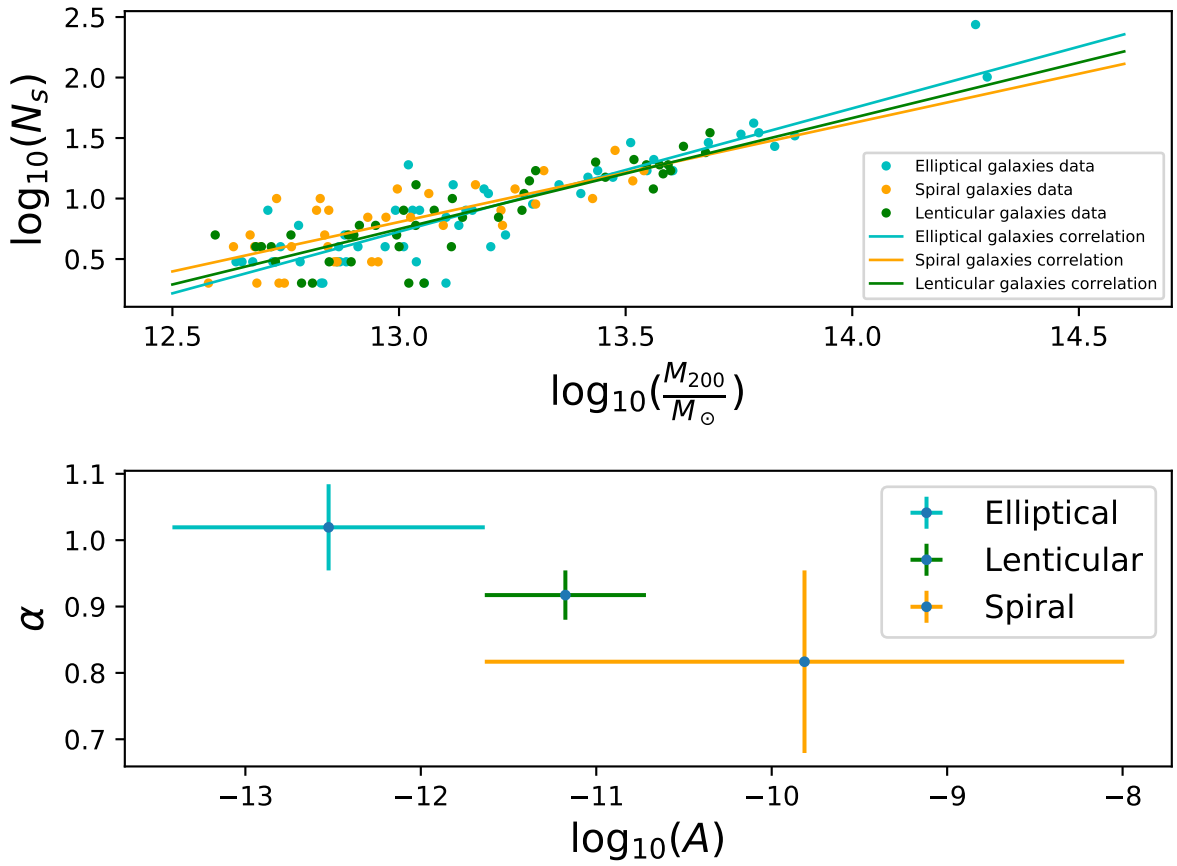

Figure 4.3: Upper figure: correlation between our samples of host galaxies and the number of their satellites. Bottom figure: the error between the linear relation of the three types of galaxies in reference with all of them.

As we can see in figure 4.4, for massive galaxies, the stellar mass of the host galaxies and the total mass of the halo, M_{200}, follow a linear relation. So, it is to be expected that the relation between the host stellar mass and the number of satellites, has a similar nature.

$$\left.\begin{array}{l}\log_{10} M_* \ \alpha \ \log_{10} M_{200} \\ \log_{10} N_s \ \alpha \ \log_{10} M_{200}\end{array}\right\} = \log_{10} N_s \ \alpha \ \log_{10} M_*$$

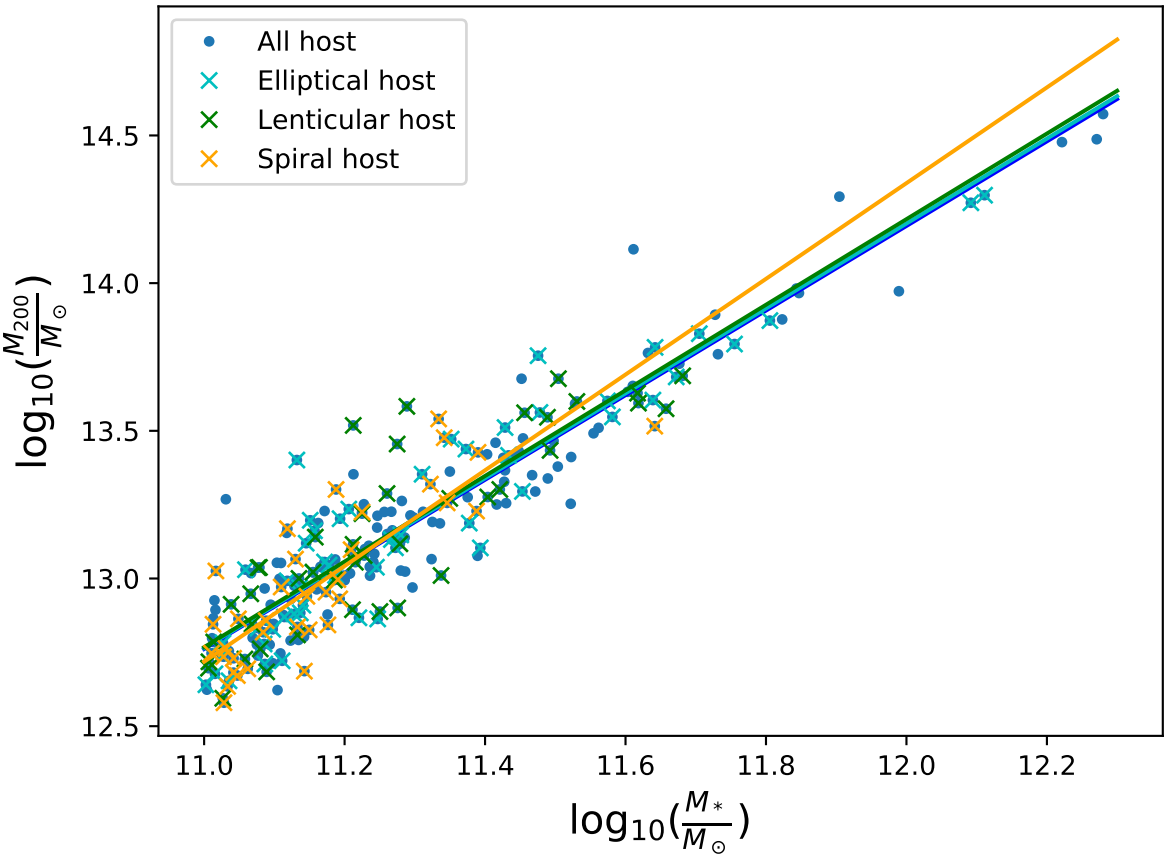

Figure 4.4: Correlation between the mass of the halo and the stellar mass of the host for the different types of galaxies.

After that, we study the amount of stellar mass accumulated by the satellites around our samples of massive galaxies within the same range of stellar mass that [Ruiz et al., 2015] used. In figure 4.5 we can see an histogram with the above relation for each morphological types. In blue, we present the elliptical galaxies, with the coloured area as the error bars obtained on the fitting. In green, we can see the same results with the lenticular galaxies, and spirals galaxies has been represented in orange. We see how the tree types overlap and therefore we cannot observe differences between the morphology. These results go against the ones obtained by [Ruiz et al., 2015] for the same mass range.

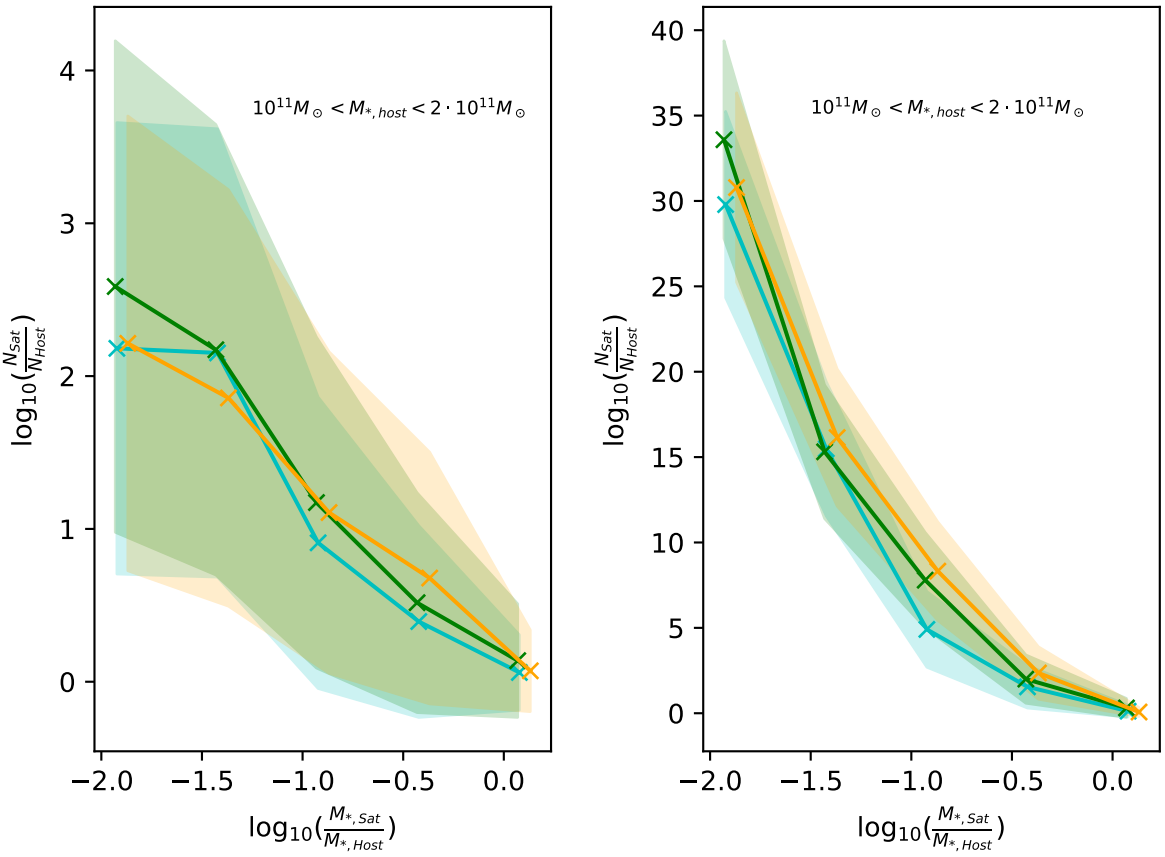

Figure 4.5: Left-hand panel: differential number of satellites per galaxy host for each morphological type versus the stellar mass ratio satellite-host. The coloured areas represent the error bars for each sample. The blue lines correspond to E-type, green to S0-type and orange to spiral type. Right-hand panel: cumulative number of satellites per galaxy host for each morphological type versus stellar mass ratio satellite-host. The colours associated with the lines and areas is the same that in the left-hand panel.

However, if we extend the stellar mass range of our host galaxies to a stellar mass larger than 10^{11} $M_\odot$ we can see how, in this case, there is a growing trend of elliptical having a large number of satellites followed by lenticular and spiral galaxies, figure 4.6. Nevertheless, as we can see in the 4.4, we have not a significant number of host galaxies with a stellar mass larger than 6×10^{11} $M_\odot$, so the statistic error is large enough to take into account this dependence.

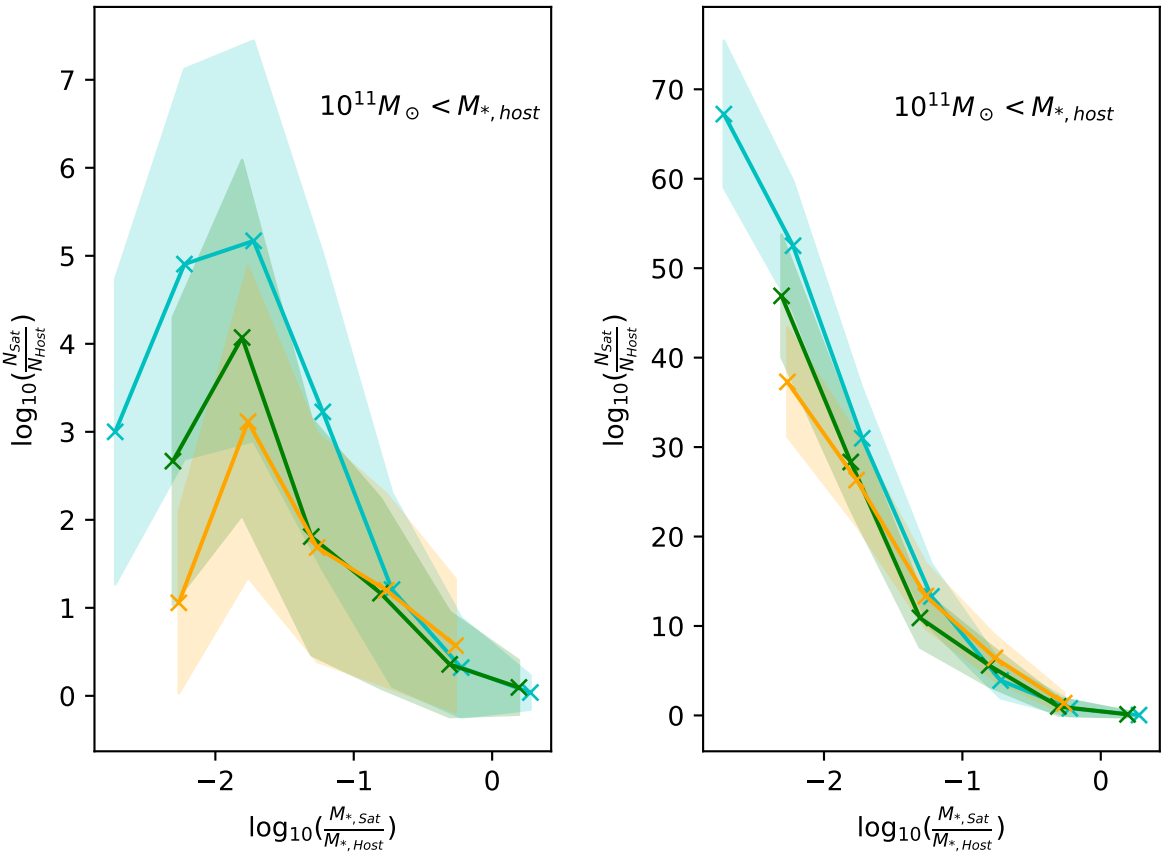

Figure 4.6: Left-hand panel: differential number of satellites per galaxy host for each morphological type versus the stellar mass ratio satellite-host. The coloured areas represent the error bars for each sample. The blue lines correspond to E-type, green to S0-type and orange to spiral type. Right-hand panel: cumulative number of satellites per galaxy host for each morphological type versus stellar mass ratio satellite-host. The colours associated with the lines and areas is the same that in the left-hand panel.

4.2 Visual insight of the galaxy host

In this section, we are going to give a visual insight to the face on and edge on projection of the host galaxies which we have studied. To do this we select 20 random galaxies from each morphological type.

These images have been generated by the method proposed with [Lupton et al., 2004] through combinations of synthetic images in bands i,r,g of the Sloan filters. Only one galaxy is represented in each image, i.e, we cannot see mergers of two galaxies or com-

panion galaxies in the images, only the remnants of said merge. In addition, there are only images belonging to galaxies with stellar masses larger than 10^{10} $M_{\odot}$ within an spherical aperture of 30 kpc. For more details of how EAGLE generated these images see [McAlpine et al., 2016] and the references inside them.

In figures 4.7 and 4.8 we present the visual edge on projection and face on projection of 20 random galaxies from 33 elliptical galaxies. Also, figures 4.9 and 4.10 show the edges on view and faces on view of 20 random galaxies from 28 lenticular morphology type and, finally, in figures 4.11 and 4.12 the visual edge on projection and face on projection of 20 random galaxies from 28 spiral samples. In these images we can see that there is contamination for each morphological type, with passive galaxies having a bigger amount compared to spirals.

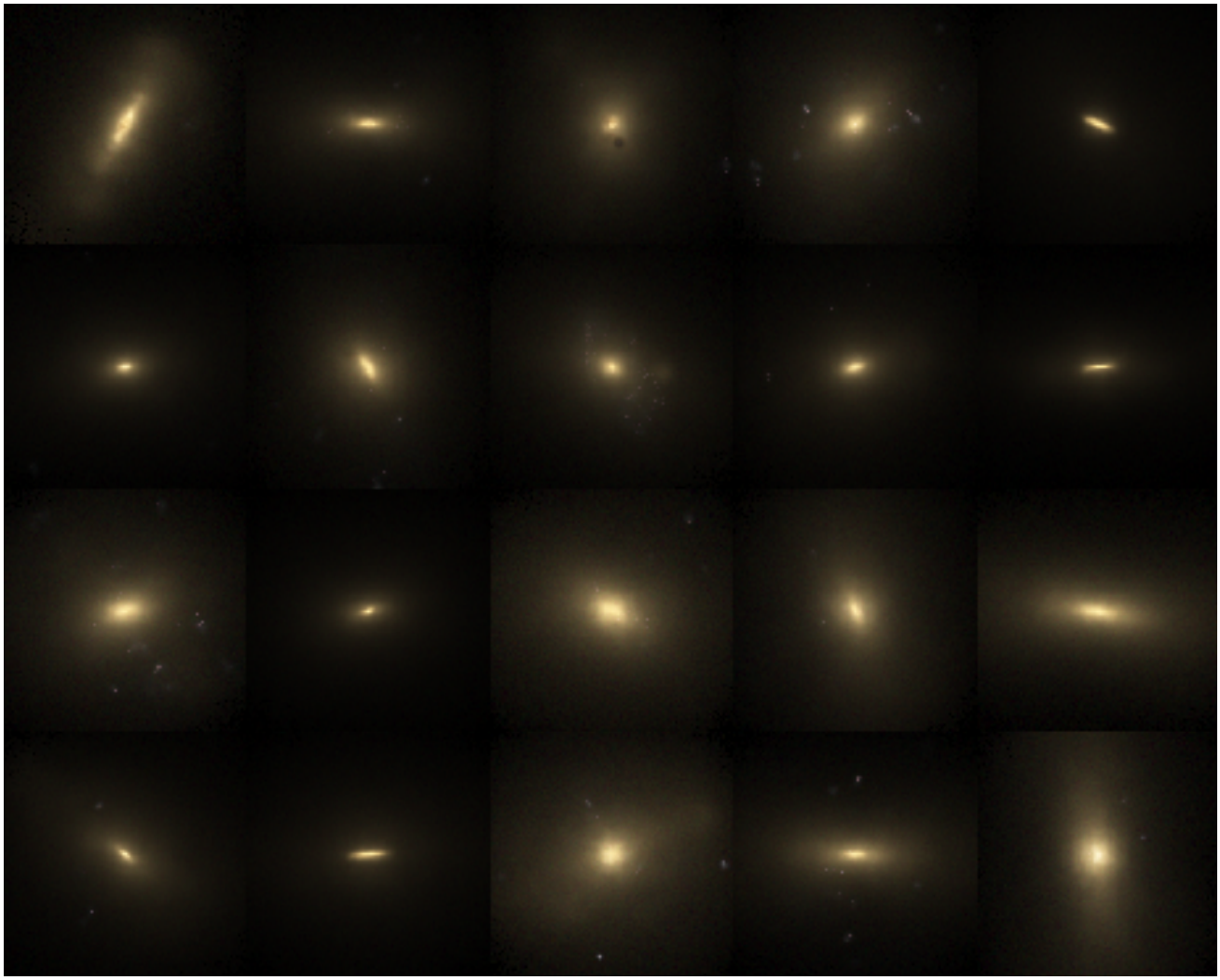

Figure 4.7: Mock gri images of elliptical galaxies in a edge on visual insight within a spherical aperture of 30 kpc. We can see galaxy host that does not follow the morphology classification with accurate.

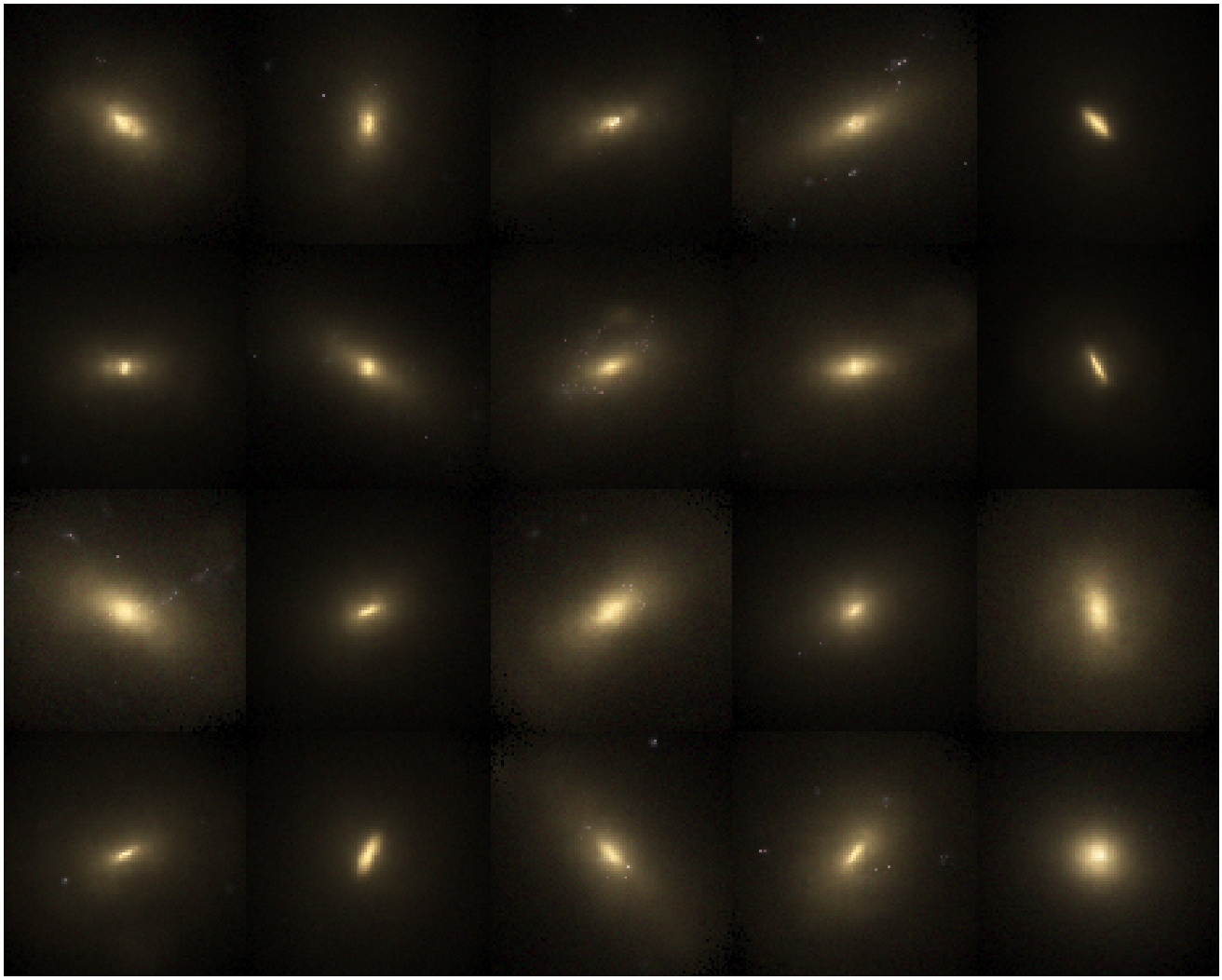

Figure 4.8: Mock gri images of elliptical galaxies in a face on view within a spherical aperture of 30 kpc. We can see galaxy host that does not follow the morphology classification with accurate.

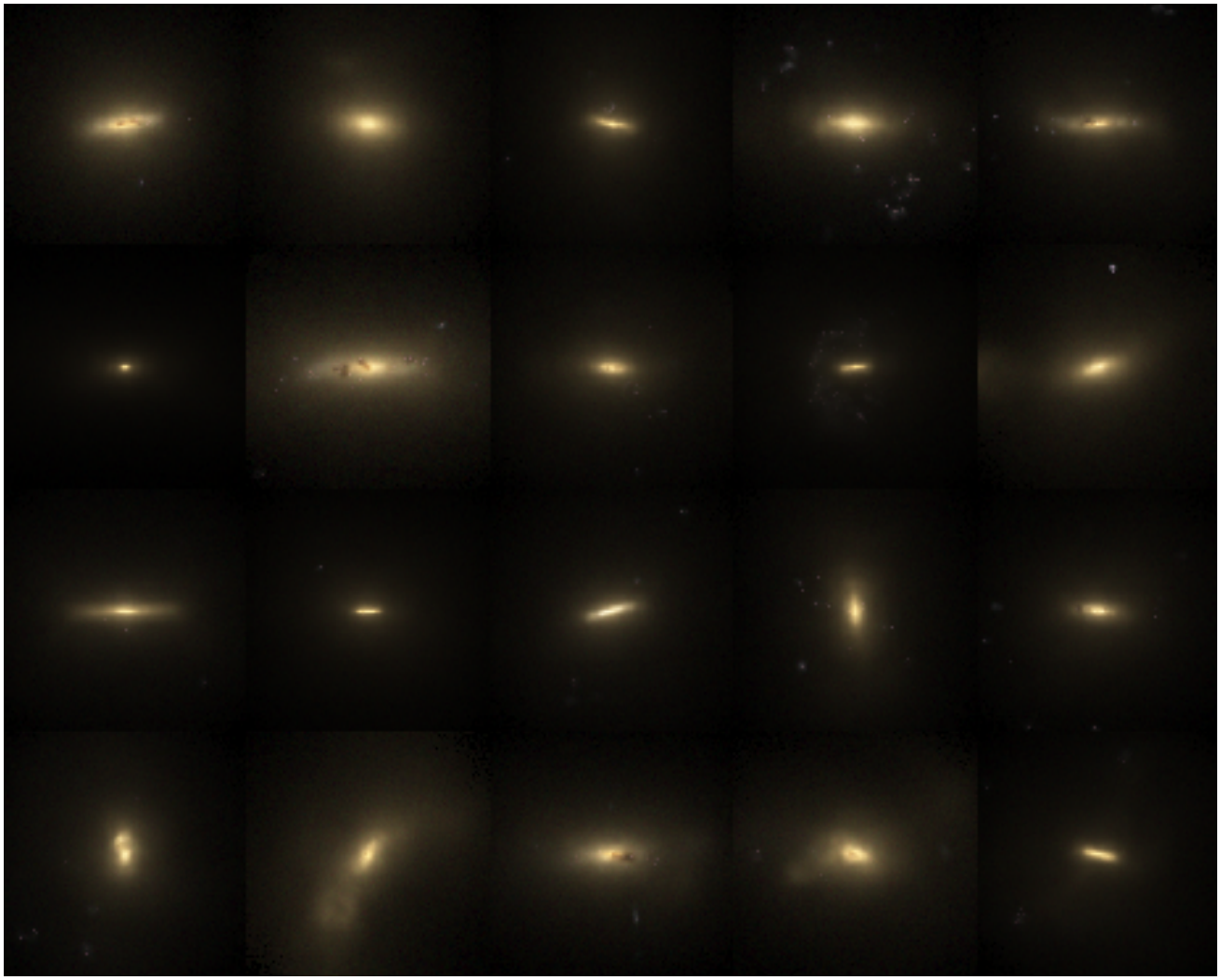

Figure 4.9: Mock gri images of lenticular galaxies in a edge on view within a spherical aperture of 30 kpc. We can see galaxy host that does not follow the morphology classification with accurate.

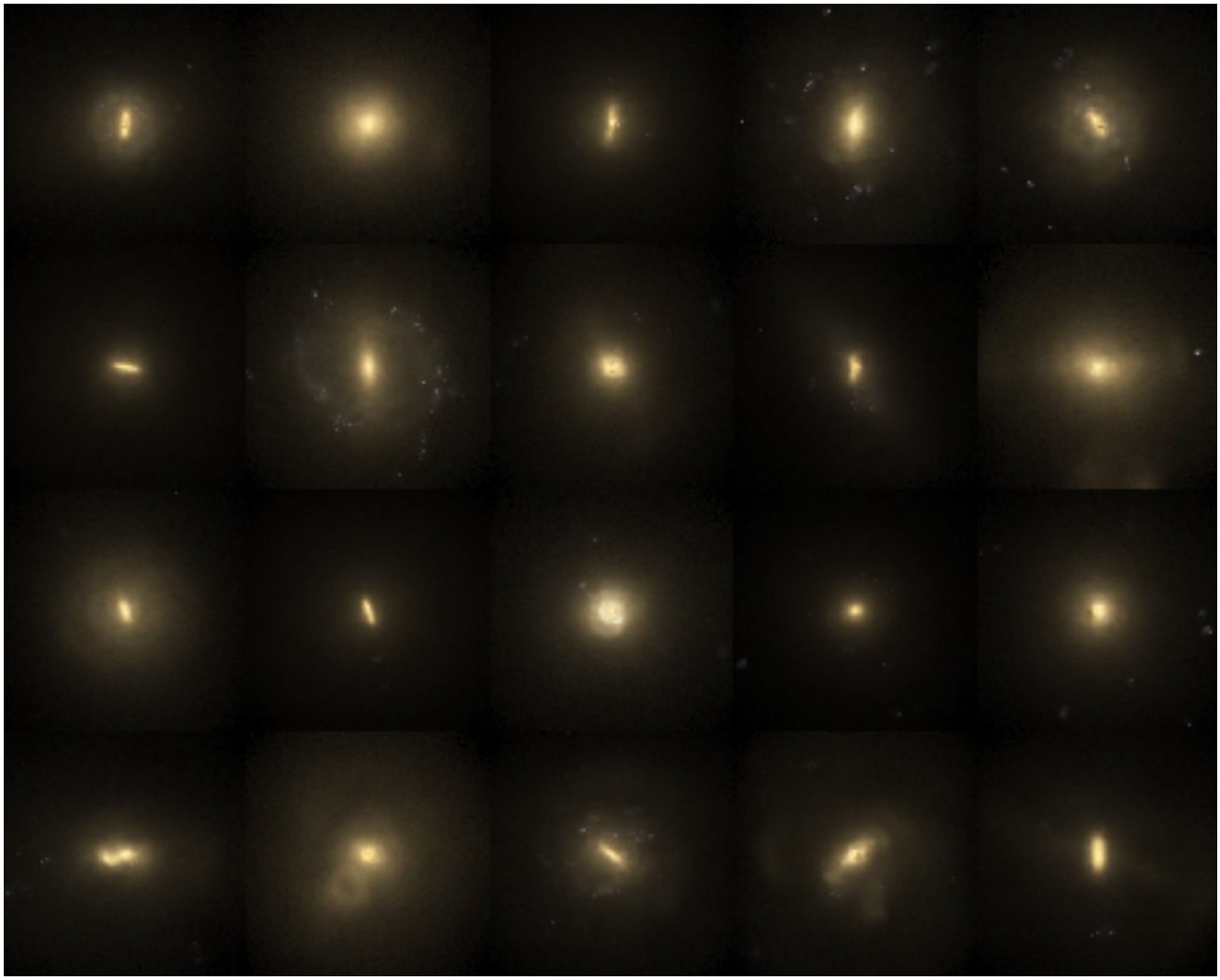

Figure 4.10: Mock gri images of lenticular galaxies in a face on view within a spherical aperture of 30 kpc. We can see galaxy host that does not follow the morphology classification with accurate.

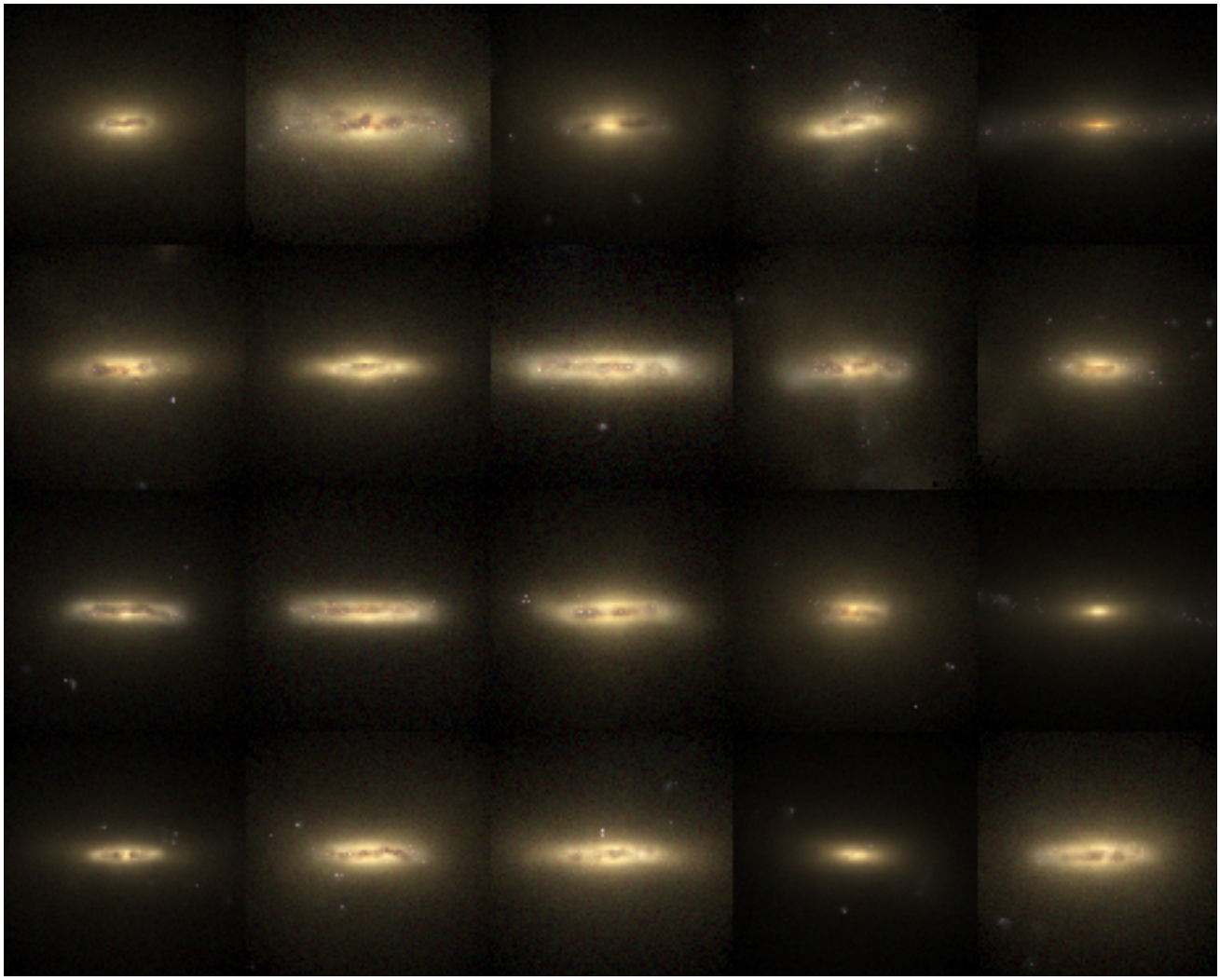

Figure 4.11: Mock gri images of spiral galaxies in a edge on view within a spherical aperture of 30 kpc. We can see galaxy host that does not follow the morphology classification with accurate.

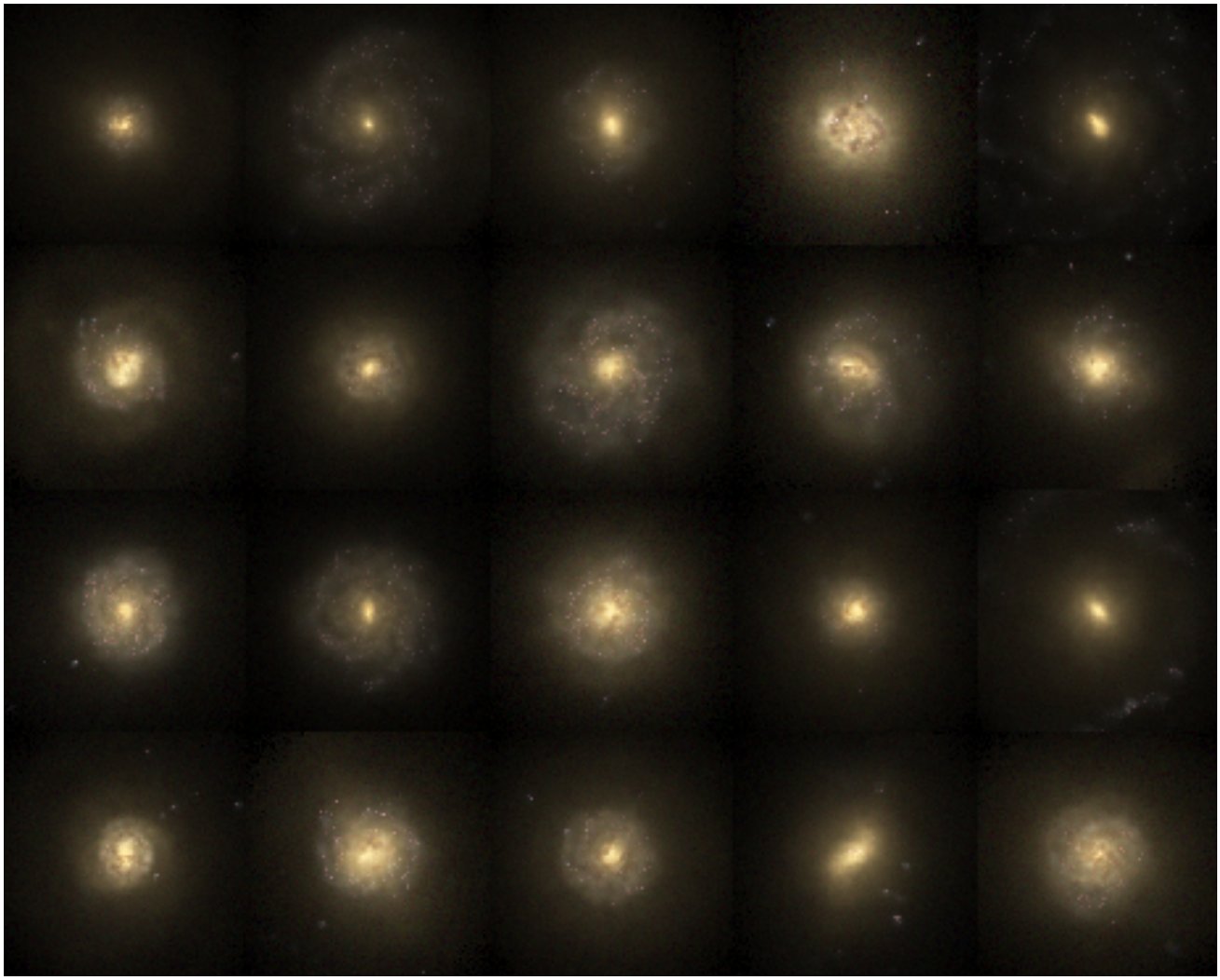

Figure 4.12: Mock gri images of spiral galaxies in a face on view within a spherical aperture of 30 kpc. We can see galaxy host that does not follow the morphology classification with accurate.

Chapter 5

Conclusions

Tras los resultados obtenidos, es posible comprobar que no existe un acuerdo entre las simulaciones y los datos observados. Con el mismo rango de masa, las observaciones apuntan que existe una fuerte dependencia del número de galaxias satélite y la morfología de la galaxia central. Sin embargo, las simulaciones no muestran dicha dependencia. Por otro lado, al aumentar el rango de masa de las galaxias centrales, se ve una pequeña tendencia a la dependencia indicada anteriormente, pero dada la poca estadística con la que trabajamos en rangos de masa tan altos, no es posible verificar este resultado. Estudios futuros podrían, con un mayor resolución, verificar o contradecir este punto.

We have studied, using the same analysis as [Ruiz et al., 2015] with observational data, the relation between the abundance of satellites and the morphology of the host galaxy with the aim to verify what seems to be the main process of galaxy formation; the galaxy mergers. For this reason, we have used a hydrodynamical simulation of EAGLE. Using several methods we have selected all massive host galaxies with a stellar mass range larger than 10^{11} $M_{\odot}$ and linked them with their respective satellites (that have a stellar mass larger than 10^{9} $M_{\odot}$). According to the morphology definition of [Sales et al., 2010] and [Romanowsky and Fall, 2012], we have classified the hosts galaxies as elliptical, spiral and lenticular types.

The statistical analysis of the correlation between the number of satellites and the morphology of the host can be summarised as follow:

- We have found that the correlation between the number of satellite galaxies per host

does not show any dependence with the morphology types, if we take into account the stellar mass range used by [Ruiz et al., 2015] for the host.

- By increasing the stellar mass range of the galaxy hosts, it is possible to find a dependence with the morphology. Nevertheless, we do not have enough data in the simulation to be able to back this statement.

- Subdividing simulated galaxies into morphological classes, as defined in observations, is a quite challenging. We have been testing different ways to classify host galaxies into morphological classes. Finally, the classification used in this work has proved to be the most loyal. Moreover, as we can see in the images in, section 4.2, there still is some contamination of the sample. We have found that a good classification for the host encounters several limitations.

- The discrepancies between this work and the observational results could be due to the observational biases introduce by the clustering and background correction.

Further work can be done with simulations with a larger number of hosts in the mass range in which we have seen a morphological dependence or with a much more accurate morphological separation. This can lead to a better understanding of the formation and evolution of galaxies, opening the doors to new ways to explain that or reaffirm the existing theories.

Chapter 6

Bibliography

[Ade et al., 2014] Ade, P. A. R., Aghanim, N., Alves, M. I. R., Armitage-Caplan, C., Arnaud, M., Ashdown, M., Atrio-Barandela, F., Aumont, J., Aussel, H., Baccigalupi, C., Banday, A. J., Barreiro, R. B., Barrena, R., Bartelmann, M., Bartlett, J. G., Bartolo, N., Basak, S., Battaner, E., Battye, R., Benabed, K., Benoît, A., Benoit-Lévy, A., Bernard, J.-P., Bersanelli, M., Bertincourt, B., Bethermin, M., Bielewicz, P., Bikmaev, I., Blanchard, A., Bobin, J., Bock, J. J., Böhringer, H., Bonaldi, A., Bonavera, L., Bond, J. R., Borrill, J., Bouchet, F. R., Boulanger, F., Bourdin, H., Bowyer, J. W., Bridges, M., Brown, M. L., Bucher, M., Burenin, R., Burigana, C., Butler, R. C., Calabrese, E., Cappellini, B., Cardoso, J.-F., Carr, R., Carvalho, P., Casale, M., Castex, G., Catalano, A., Challinor, A., Chamballu, A., Chary, R.-R., Chen, X., Chiang, H. C., Chiang, L.-Y., Chon, G., Christensen, P. R., Churazov, E., Church, S., Clemens, M., Clements, D. L., Colombi, S., Colombo, L. P. L., Combet, C., Comis, B., Couchot, F., Coulais, A., Crill, B. P., Cruz, M., Curto, A., Cuttaia, F., Da Silva, A., Dahle, H., Danese, L., Davies, R. D., Davis, R. J., de Bernardis, P., de Rosa, A., de Zotti, G., Déchelette, T., Delabrouille, J., Delouis, J.-M., Démoclès, J., Désert, F.-X., Dick, J., Dickinson, C., Diego, J. M., Dolag, K., Dole, H., Donzelli, S., Doré, O., Douspis, M., Ducout, A., Dunkley, J., Dupac, X., Efstathiou, G., Elsner, F., Enßlin, T. A., Eriksen, H. K., Fabre, O., Falgarone, E., Falvella, M. C., Fantaye, Y., Fergusson, J., Filliard, C., Finelli, F., Flores-Cacho, I., Foley, S., Forni, O., Fosalba, P., Frailis, M., Fraisse, A. A., Franceschi, E., Freschi, M., Fromenteau, S., Frommert, M., Gaier, T. C., Galeotta, S., Gallegos, J., Galli, S., Gandolfo, B., Ganga, K., Gauthier, C., Génova-Santos, R. T., Ghosh, T., Giard, M., Giardino, G., Gilfanov, M., Girard, D., Giraud-Héraud, Y., Gjerløw, E., González-Nuevo, J., Górski, K. M., Gratton, S., Gregorio, A., Gruppuso, A., Gudmundsson, J. E., Haissinski, J., Hamann, J., Hansen, F. K., Hansen, M.,

Hanson, D., Harrison, D. L., Heavens, A., Helou, G., Hempel, A., Henrot-Versillé, S., Hernández-Monteagudo, C., Herranz, D., Hildebrandt, S. R., Hivon, E., Ho, S., Hobson, M., Holmes, W. A., Hornstrup, A., Hou, Z., Hovest, W., Huey, G., Huffenberger, K. M., Hurier, G., Ilić, S., Jaffe, A. H., Jaffe, T. R., Jasche, J., Jewell, J., Jones, W. C., Juvela, M., Kalberla, P., Kangaslahti, P., Keihänen, E., Kerp, J., Keskitalo, R., Khamitov, I., Kiiveri, K., Kim, J., Kisner, T. S., Kneissl, R., Knoche, J., Knox, L., Kunz, M., Kurki-Suonio, H., Lacasa, F., Lagache, G., Lähteenmäki, A., Lamarre, J.-M., Langer, M., Lasenby, A., Lattanzi, M., Laureijs, R. J., Lavabre, A., Lawrence, C. R., Le Jeune, M., Leach, S., Leahy, J. P., Leonardi, R., León-Tavares, J., Leroy, C., Lesgourgues, J., Lewis, A., Li, C., Liddle, A., Liguori, M., Lilje, P. B., Linden-Vørnle, M., Lindholm, V., López-Caniego, M., Lowe, S., Lubin, P. M., Macías-Pérez, J. F., MacTavish, C. J., Maffei, B., Maggio, G., Maino, D., Mandolesi, N., Mangilli, A., Marcos-Caballero, A., Marinucci, D., Maris, M., Marleau, F., Marshall, D. J., Martin, P. G., Martínez-González, E., Masi, S., Massardi, M., Matarrese, S., Matsumura, T., Matthai, F., Maurin, L., Mazzotta, P., McDonald, A., McEwen, J. D., McGehee, P., Mei, S., Meinhold, P. R., Melchiorri, A., Melin, J.-B., Mendes, L., Menegoni, E., Mennella, A., Migliaccio, M., Mikkelsen, K., Millea, M., Miniscalco, R., Mitra, S., Miville-Deschênes, M.-A., Molinari, D., Moneti, A., Montier, L., Morgante, G., Morisset, N., Mortlock, D., Moss, A., Munshi, D., Murphy, J. A., Naselsky, P., Nati, F., Natoli, P., Negrello, M., Nesvadba, N. P. H., Netterfield, C. B., Nørgaard-Nielsen, H. U., North, C., Noviello, F., Novikov, D., Novikov, I., O'Dwyer, I. J., Orieux, F., Osborne, S., O'Sullivan, C., Oxborrow, C. A., Paci, F., Pagano, L., Pajot, F., Paladini, R., Pandolfi, S., Paoletti, D., Partridge, B., Pasian, F., Patanchon, G., Paykari, P., Pearson, D., Pearson, T. J., Peel, M., Peiris, H. V., Perdereau, O., Perotto, L., Perrotta, F., Pettorino, V., Piacentini, F., Piat, M., Pierpaoli, E., Pietrobon, D., Plaszczynski, S., Platania, P., Pogosyan, D., Pointecouteau, E., Polenta, G., Ponthieu, N., Popa, L., Poutanen, T., Pratt, G. W., Prézeau, G., Prunet, S., Puget, J.-L., Pullen, A. R., Rachen, J. P., Racine, B., Rahlin, A., Räth, C., Reach, W. T., Rebolo, R., Reinecke, M., Remazeilles, M., Renault, C., Renzi, A., Riazuelo, A., Ricciardi, S., Riller, T., Ringeval, C., Ristorcelli, I., Robbers, G., Rocha, G., Roman, M., Rosset, C., Rossetti, M., Roudier, G., Rowan-Robinson, M., Rubiño-Martín, J. A., Ruiz-Granados, B., Rusholme, B., Salerno, E., Sandri, M., Sanselme, L., Santos, D., Savelainen, M., Savini, G., Schaefer, B. M., Schiavon, F., Scott, D., Seiffert, M. D., Serra, P., Shellard, E. P. S., Smith, K., Smoot, G. F., Souradeep, T., Spencer, L. D., Starck, J.-L., Stolyarov, V., Stompor, R., Sudiwala, R., Sunyaev, R., Sureau, F., Sutter, P., Sutton, D., Suur-Uski, A.-S., Sygnet, J.-F., Tauber, J. A.,

Tavagnacco, D., Taylor, D., Terenzi, L., Texier, D., Toffolatti, L., Tomasi, M., Torre, J.-P., Tristram, M., Tucci, M., Tuovinen, J., Türler, M., Tuttlebee, M., Umana, G., Valenziano, L., Valiviita, J., Van Tent, B., Varis, J., Vibert, L., Viel, M., Vielva, P., Villa, F., Vittorio, N., Wade, L. A., Wandelt, B. D., Watson, C., Watson, R., Wehus, I. K., Welikala, N., Weller, J., White, M., White, S. D. M., Wilkinson, A., Winkel, B., Xia, J.-Q., Yvon, D., Zacchei, A., Zibin, J. P., and Zonca, A. (2014). Planck 2013 results. I. Overview of products and scientific results. *Astronomy & Astrophysics*, 571:A1.

[Bournaud et al., 2011] Bournaud, F., Chapon, D., Teyssier, R., Powell, L. C., Elmegreen, B. G., Elmegreen, D. M., Duc, P.-A., Contini, T., Epinat, B., and Shapiro, K. L. (2011). HYDRODYNAMICS OF HIGH-REDSHIFT GALAXY COLLISIONS: FROM GAS-RICH DISKS TO DISPERSION-DOMINATED MERGERS AND COMPACT SPHEROIDS. *The Astrophysical Journal*, 730(1):4.

[Crain et al., 2015] Crain, R. A., Schaye, J., Bower, R. G., Furlong, M., Schaller, M., Theuns, T., Dalla Vecchia, C., Frenk, C. S., McCarthy, I. G., Helly, J. C., Jenkins, A., Rosas-Guevara, Y. M., White, S. D. M., and Trayford, J. W. (2015). The EAGLE simulations of galaxy formation: calibration of subgrid physics and model variations. *Monthly Notices of the Royal Astronomical Society*, 450(2):1937–1961.

[Croft et al., 1998] Croft, R. A. C., Weinberg, D. H., Katz, N., and Hernquist, L. (1998). Recovery of the Power Spectrum of Mass Fluctuations from Observations of the Lyα Forest. *The Astrophysical Journal*, 495(1):44–62.

[Davis et al., 1985] Davis, M., Efstathiou, G., Frenk, C. S., and White, S. D. M. (1985). The evolution of large-scale structure in a universe dominated by cold dark matter. *The Astrophysical Journal*, 292:371.

[Dekel et al., 2009] Dekel, A., Birnboim, Y., Engel, G., Freundlich, J., Goerdt, T., Mumcuoglu, M., Neistein, E., Pichon, C., Teyssier, R., and Zinger, E. (2009). Cold streams in early massive hot haloes as the main mode of galaxy formation. *Nature*, 457(7228):451–454.

[Díaz-García et al., 2013] Díaz-García, L. A., Mármol-Queraltó, E., Trujillo, I., Cenarro, A. J., López-Sanjuan, C., Pérez-González, P. G., and Barro, G. (2013). The merger history of massive spheroids since z 1 is size-independent. *Monthly Notices of the Royal Astronomical Society*, 433(1):60–68.

[Dolag et al., 2009] Dolag, K., Borgani, S., Murante, G., and Springel, V. (2009). Substructures in hydrodynamical cluster simulations. *Monthly Notices of the Royal Astronomical Society*, 399(2):497–514.

[Dressler, 1980] Dressler, A. (1980). Galaxy morphology in rich clusters - Implications for the formation and evolution of galaxies. *The Astrophysical Journal*, 236:351.

[Hubble, 1926] Hubble, E. P. (1926). Extragalactic nebulae. *The Astrophysical Journal*, 64:321.

[Javier Cenarro and Trujillo, 2009] Javier Cenarro, A. and Trujillo, I. (2009). MILD VELOCITY DISPERSION EVOLUTION OF SPHEROID-LIKE MASSIVE GALAXIES SINCE z 2. *The Astrophysical Journal*, 696(1):L43–L47.

[Jenkins, 2010] Jenkins, A. (2010). Second-order Lagrangian perturbation theory initial conditions for resimulations. *Monthly Notices of the Royal Astronomical Society*, 403(4):1859–1872.

[Kennicutt, Jr., 1998] Kennicutt, Jr., R. C. (1998). The Global Schmidt Law in Star-forming Galaxies. *The Astrophysical Journal*, 498(2):541–552.

[Kereš et al., 2005] Kereš, D., Katz, N., Weinberg, D. H., and Davé, R. (2005). How do galaxies get their gas? *Monthly Notices of the Royal Astronomical Society*, 363(1):2–28.

[Khochfar and Silk, 2006] Khochfar, S. and Silk, J. (2006). A simple model for the size-evolution of elliptical galaxies.

[Lupton et al., 2004] Lupton, R., Blanton, M. R., Fekete, G., Hogg, D. W., O'Mullane, W., Szalay, A., and Wherry, N. (2004). Preparing Red-Green-Blue Images from CCD Data. *Publications of the Astronomical Society of the Pacific*, 116(816):133–137.

[McAlpine et al., 2016] McAlpine, S., Helly, J. C., Schaller, M., Trayford, J. W., Qu, Y., Furlong, M., Bower, R. G., Crain, R. A., Schaye, J., Theuns, T., Dalla Vecchia, C., Frenk, C. S., McCarthy, I. G., Jenkins, A., Rosas-Guevara, Y., White, S. D., Baes, M., Camps, P., and Lemson, G. (2016). The eagle simulations of galaxy formation: Public release of halo and galaxy catalogues. *Astronomy and Computing*, 15:72–89.

[McDonald et al., 2005] McDonald, P., Seljak, U., Cen, R., Shih, D., Weinberg, D. H., Burles, S., Schneider, D. P., Schlegel, D. J., Bahcall, N. A., Briggs, J. W., Brinkmann, J., Fukugita, M., Ivezić, Ž., Kent, S., and Vanden Berk, D. E. (2005). The Linear

Theory Power Spectrum from the Lyα Forest in the Sloan Digital Sky Survey. *The Astrophysical Journal*, 635(2):761–783.

[Oser et al., 2012] Oser, L., Naab, T., Ostriker, J. P., and Johansson, P. H. (2012). THE COSMOLOGICAL SIZE AND VELOCITY DISPERSION EVOLUTION OF MASSIVE EARLY-TYPE GALAXIES. *The Astrophysical Journal*, 744(1):63.

[Oser et al., 2010] Oser, L., Ostriker, J. P., Naab, T., Johansson, P. H., and Burkert, A. (2010). THE TWO PHASES OF GALAXY FORMATION. *The Astrophysical Journal*, 725(2):2312–2323.

[Ricciardelli et al., 2010] Ricciardelli, E., Trujillo, I., Buitrago, F., and Conselice, C. J. (2010). The evolutionary sequence of submillimetre galaxies: from diffuse discs to massive compact ellipticals? *Monthly Notices of the Royal Astronomical Society*, 406(1):230–236.

[Romanowsky and Fall, 2012] Romanowsky, A. J. and Fall, S. M. (2012). ANGULAR MOMENTUM AND GALAXY FORMATION REVISITED. *The Astrophysical Journal Supplement Series*, 203(2):17.

[Ruiz et al., 2015] Ruiz, P., Trujillo, I., and Mármol-Queraltó, E. (2015). The abundance of satellites depends strongly on the morphology of the host galaxy. *Monthly Notices of the Royal Astronomical Society*, 454(2):1605–1619.

[Sales et al., 2010] Sales, L. V., Navarro, J. F., Schaye, J., Vecchia, C. D., Springel, V., and Booth, C. M. (2010). Feedback and the structure of simulated galaxies at redshift z= 2. *Monthly Notices of the Royal Astronomical Society*, 409(4):1541–1556.

[Schaye, 2004] Schaye, J. (2004). Star Formation Thresholds and Galaxy Edges: Why and Where. *The Astrophysical Journal*, 609(2):667–682.

[Schaye et al., 2015] Schaye, J., Crain, R. A., Bower, R. G., Furlong, M., Schaller, M., Theuns, T., Dalla Vecchia, C., Frenk, C. S., Mccarthy, I. G., Helly, J. C., Jenkins, A., Rosas-Guevara, Y. M., White, S. D., Baes, M., Booth, C. M., Camps, P., Navarro, J. F., Qu, Y., Rahmati, A., Sawala, T., Thomas, P. A., and Trayford, J. (2015). The EAGLE project: Simulating the evolution and assembly of galaxies and their environments. *Monthly Notices of the Royal Astronomical Society*, 446(1):521–554.

[Schaye and Dalla Vecchia, 2008] Schaye, J. and Dalla Vecchia, C. (2008). On the relation between the Schmidt and Kennicutt–Schmidt star formation laws and its implications for

numerical simulations. *Monthly Notices of the Royal Astronomical Society*, 383(3):1210–1222.

[Schaye et al., 2000] Schaye, J., Theuns, T., Rauch, M., Efstathiou, G., and Sargent, W. L. (2000). The thermal history of the intergalactic medium. *Monthly Notices of the Royal Astronomical Society*, 318(3):817–826.

[Springel et al., 2001] Springel, V., White, S. D. M., Tormen, G., and Kauffmann, G. (2001). Populating a cluster of galaxies – I. Results at z = 0. *Monthly Notices of the Royal Astronomical Society*, 328(3):726–750.

[Summers et al., 1995] Summers, F. J., Davis, M., and Evrard, A. E. (1995). Galaxy Tracers and Velocity Bias.

[The EAGLE team, 2017] The EAGLE team (2017). The EAGLE simulations of galaxy formation: Public release of particle data. pages 1–20.

[Tinker et al., 2008] Tinker, J., Kravtsov, A. V., Klypin, A., Abazajian, K., Warren, M., Yepes, G., Gottlöber, S., and Holz, D. E. (2008). Toward a Halo Mass Function for Precision Cosmology: The Limits of Universality. *The Astrophysical Journal*, 688(2):709–728.

[Trujillo et al., 2011] Trujillo, I., Ferreras, I., and de la Rosa, I. G. (2011). Dissecting the size evolution of elliptical galaxies since z 1: puffing-up versus minor-merging scenarios. *Monthly Notices of the Royal Astronomical Society*, 415(4):3903–3913.

[Viel et al., 2004] Viel, M., Haehnelt, M. G., and Springel, V. (2004). Inferring the dark matter power spectrum from the Lyman α forest in high-resolution QSO absorption spectra. *Monthly Notices of the Royal Astronomical Society*, 354(3):684–694.

[Wuyts et al., 2010] Wuyts, S., Cox, T. J., Hayward, C. C., Franx, M., Hernquist, L., Hopkins, P. F., Jonsson, P., and van Dokkum, P. G. (2010). ON SIZES, KINEMATICS,M/L GRADIENTS, AND LIGHT PROFILES OF MASSIVE COMPACT GALAXIES ATz$˜$ 2. *The Astrophysical Journal*, 722(2):1666–1684.